Estimation and classification of background-induced errors on a trapped ion qubit network through a probabilistic graphical model

Chung Daun [*1,2] **Kang Jiyong** [*1,2] **Lee Kyungmin** [*1,2]

Abstract

Probabilistic graphical models (PGM) can be applied to the understanding of the physics of trapped-ion quantum computing systems. An atomic qubit, or quantum bit, is described by multiple degrees-of-freedom that must be controlled with great precision in order to qualify as a quantum information carrier. It is hard to solve the dynamics of a trapped-ion qubit in the presence of background error sources in an analytical fashion. While performing numerical simulations become an essential task, increasing computational complexity often hinders the intuitive interpretation of the underlying model. In this work, we use a probabilistic graphical model-style approach to simplify the zoo of interactions involved in trapped-ion manipulations into a tractable form. Application to experimental data shows that our approach can serve as an alternative to the standard methods used for extracting the heating rate of a trapped-ion.

1. Introduction

1.1. Problem Definition and Motivation

Trapped-ion systems are great candidate platforms for quantum computation due to their natural stability. The information carriers of the system are charged atoms trapped in oscillating electric fields. The atoms are described by mainly two degrees-of-freedom: the internal and motional states. The internal states are the actual qubit states $|0\rangle$ and $|1\rangle$ which in general can be in superposition $\psi|0\rangle = \alpha|0\rangle + \beta|0\rangle$. The motional states are harmonic oscillator states, which are induced by the fact that the qubit is trapped in a harmonic potential well. These states are used as mediators of interaction between the internal states of distinct qubits. External laser signals can be used to couple these two degrees-of-freedom. For example, two laser beams can be shined on different ions to transform them into an entangled state. A schematic representation of the trapped ion qubit is given in Figure 1 (a). Here we also include a heat bath that can scramble the motional states by a process called heating or damping. Since external laser fields couple internal and motional states to perform quantum gates, such heating process eventually causes the coherence of the internal states to decay. That is, the qubit loses its quantum behavior and becomes submerged in classical noise. Measurement of this heating rate is vital in characterising the quality of an experimental trapped-ion system. In this work, we present a graphical representation of the heating of an ion and the subsequent decay of the qubit state. Although the dynamics can be modeled using differential equations only, the meanings of the physical interactions and marginalization processes at certain stages became clearer when applying a PGM-style interpretation. Also, we argue that our model can extract the heating rate from experimental data in a more simple manner compared to conventional methods.

1.2. Related work

The difficulty of both modeling and measuring the motional properties and its influences on the internal state of the qubit lies in the fact that one cannot observe the motional state directly. The data that is observed in trapped-ion experiments is exclusively based on internal states. This is because they are much easier to detect, and their signals leave fingerprints of the underlying motional states, so that one can make inferences about them indirectly. The quantum behavior of the internal state is captured in the Rabi flopping phenomenon where the probability of the internal $|1\rangle$ state oscillates between zero and one in response to the applied laser signal. Decay patterns emerge when the internal states are influenced by damped motional states. The decay is effectively parameterized by what is known as the heating rate. The standard method for measuring the heating rates in trapped-ion systems is to measure the response of the ion to the so-called red- and blue-sideband lasers (C. Monroe et al., 1995; Leibfried et al., 1996; R. J. Epstein et al., 2007). The red- and blue-sideband lasers are lasers that are tuned from the carrier frequency of the internal state transition

[*]Equal contribution [1]Department of CSE, Seoul National University, Seoul, Korea. [2]Team 5, PGM Lecture, 2022, SNU. Correspondence to: Chung Daun <acornzet@snu.ac.kr>, Kang Jiyong <kangz12345@snu.ac.kr>, Lee Kyungmin <anfry15rudals@snu.ac.kr>.

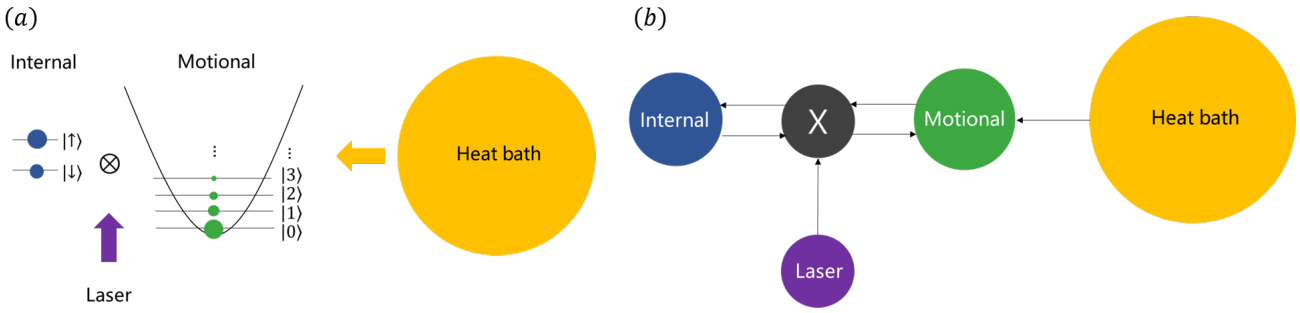

Figure 1. (a) The experimental setup for our entire quantum system. The environment is considered as a huge Heat bath and the laser induces coupling between internal (i.e. spin) states and motional states of our trapped ion quantum system. (b) The graphical modeling of our experimental setup shown in (a).

by the motional harmonic oscillator resonance frequencies, the former being $\omega_{\text{rsb}} = \omega_{\text{carrier}} - \omega_{\text{resonance}}$, and the latter $\omega_{\text{bsb}} = \omega_{\text{carrier}} + \omega_{\text{resonance}}$. These approaches share the same process of comparing the the differential responses to the red- and blue-sidebands in an iterative manner and plugging them into an approximate approximate formula to obtain the heating rate. It will be shown that our approach can extract the heating rate by using the carrier transition only, and that it does not apply any form of approximations. In the following section, we present the method used to define our graphical representation of trapped-ion dynamics. Then, simulation results and applications to experimental data are presented. Finally, we provide a conclusion.

2. Method

In this section, we introduce the equation that describes the stochastic evolution of our quantum system of interest, which is often called a master equation. We also introduce the derivation of simplified master equation using graphical model, and the numerical method we used to solve the master equation. Fist, we derive the general representation of our system using standard form of master equation for quantum system. Then, we introduce some assumptions and graphical interpretations of our system that enables us to more simplify the derived equation. We also describe the numerical method we used to solve the derived master equation of our system and further applications.

2.1. Dynamics of Trapped Ion Quantum System

A single trapped ion can be represented by two degree of freedom, the spin and motional states. In the experimental setup, there exists thermal radiations that acts on the motional states of ion and laser operations which transforms the spin states of ion. Therefore, we can define the entire system as a closed quantum system, including both trapped ion and the environment. As the evolution of closed quantum system can be represented by a system Hamiltonian, $H_{SB}(t)$, we can represents the coupling between our system of interest (the states of trapped ion) and the environment, which is often considered as a kind of heat bath, in the interaction picture as below.

$$H_{SB}(t) \equiv i\hbar(b^\dagger(t)c - b(t)c^\dagger$$

$$b(t) \equiv \frac{1}{\sqrt{2\pi}} \int_{\omega_0-\theta}^{\omega_0+\theta} d\omega db(\omega) e^{-i(\omega-\omega_0)t}$$

Here, $c, c^\dagger$ are annihilation and creation operators act on environment. With the rotating wave approximation and Born-Markov approximation, we can further represents $b(t)$ as below.

$$b(t) \equiv \frac{1}{\sqrt{2\pi}} \int_{-\infty}^{\infty} d\omega db(\omega) e^{-i(\omega-\omega_0)t}$$

Here, ω_0 corresponds to the largest energy (i.e. defines the fastest time scale) throughout the entire dynamics and the time step dt should satisfy $dt \gg 1/\theta$ due to effective theory.

Like the thermal bath in the classical case, the environment acts on the motional state of our system of interest and incurs a damping effect. With the damping constant Γ, we can define a noise operator (i.e. the Ito increment) as below.

$$B(t) \equiv \frac{1}{\sqrt{\Gamma}} \int_0^t ds db(s)$$

Using this, we can construct the stochastic Schrodinger equation for a system in a thermal bath with external coherent signals as below(Strunz, 1996; P. Zoller & Walls, 1987).

$$d|\Psi(t)\rangle = K|\Psi(t)\rangle + dB^\dagger(t)J|\Psi(t)\rangle - dB(t)J^\dagger|\Psi(t)\rangle$$

The Ito rules are given as

$$dB(t)dB^\dagger(t) = (\bar{n}_T(\omega_0) + 1)dt$$

$$dB^\dagger(t)dB(t) = \bar{n}_T(\omega_0)dt$$

Here, the drift operator K and the diffusion operator J are defined like below.

$$\begin{aligned} K &= -\frac{i}{\hbar}H_{eff}, \quad J = \sqrt{\Gamma}c \\ H_{eff} &= H'_S + \hbar(\delta\omega^- c^\dagger c - \delta\omega^+ cc^\dagger) \\ &\quad - i\hbar\frac{\Gamma}{2}\left[\bar{n}_T(\omega_0)+1)c^\dagger c + \bar{n}_T(\omega_0)cc^\dagger\right] \end{aligned}$$

Here, $\delta\omega^- c^\dagger c - \delta\omega^+ cc^\dagger$ is line-shift term and H'_S is system Hamiltonian. Then we can obtain the density matrix based evolution equation (i.e. the master equation) for our system of interest using the definition of reduced density matrix.

$$d\bar{\rho}(t) = Tr_B\{d(|\Psi(t)\rangle\langle\Psi(t)|)\}$$

Here, $\bar{\rho}$ is reduced density matrix that represents the internal degree of freedom (i.e. the spin and motional states) of our trapped ion quantum system. The master equation for $\bar{\rho}$ can be represented in the Lindblad form.

$$\begin{aligned} \frac{d\bar{\rho}(t)}{dt} &= -\frac{i}{\hbar}\left[H'_S, \bar{\rho}(t)\right] - i\left[\delta\omega^- c^\dagger c - \delta\omega^+ cc^\dagger, \bar{\rho}(t)\right] \\ &\quad - \frac{\Gamma}{2}(\bar{n}_T(\omega_0)+1)(c^\dagger c\bar{\rho}(t) + \bar{\rho}(t)c^\dagger c - 2c\bar{\rho}(t)c^\dagger) \\ &\quad - \frac{\Gamma}{2}\bar{n}_T(\omega_0)(cc^\dagger\bar{\rho}(t) + \bar{\rho}(t)cc^\dagger - 2c^\dagger\bar{\rho}(t)c) \end{aligned}$$

This is somewhat a general form of master equation describing the dynamics of our quantum system interacting with an environment as thermal bath.

2.2. Derivation of ODE for Spin States

In the previous section, we have the master equation that describes the evolution of our quantum system by tracing out the environment. To go further, we need to more specify the process which our quantum system undergoes. As we are interested in the process where the laser induces the transition of spin states of our trapped ion while the motional states are diffused due to the thermal bath, $c, c^\dagger$ are operators that acts on motional states of our system of interest. Therefore, we can represents the states of our trapped ion system as product of density operators where each stands for spin and motional states.

$$\bar{\rho} = \sum_{m,n}\bar{\rho}^{(m,n)}(t)\otimes|m\rangle\langle n|$$

However, the coupled representation of our system makes it difficult for us to construct the evolution equation related to our spin internal states, which we can only observe in the real experiments. The experimental setup is depicted in Figure 1, and it shows that the coupling induced by laser complicates the dynamics. Fortunately, the graphical model gives us insights that enables us to further derive the evolution equation for spin states of our quantum system.

Like shown in Figure 2.(a), the conditioning on the motional state of our quantum states decouples the dynamical relation between internal spin and motional states and induces more simplified graphical structure representing the dynamics of the internal spin states. Using this representation, we can derive the evolution equation for internal spin states of our quantum system corresponds to specific motional elements m, n. By sandwitching over $d\bar{\rho}/dt$ with respect to the motional states m, n we can obtain an equation that describes the evolution of internal spin states of our quantum system in the form of reduced density matrix.

$$\begin{aligned} &\frac{d\bar{\rho}^{(m,n)}(t)}{dt} = \langle m|\frac{d\bar{\rho}(t)}{dt}|n\rangle \\ &= -\frac{i}{\hbar}\left[\sum_r H'_{Sm,r}\bar{\rho}^{(r,n)}(t) - \sum_l \bar{\rho}^{(m,l)}(t)H'_{Sl,n}\right] \\ &- \frac{\Gamma}{2}\left[(2\bar{n}_T(\omega_0)+1)(m+n) + 2\bar{n}_T(\omega_0)\right]\bar{\rho}^{(m,n)}(t) \\ &+ \Gamma(\bar{n}_T(\omega_0)+1)\sqrt{(m+1)(n+1)}\bar{\rho}^{(m+1,n+1)}(t) \\ &+ \Gamma\bar{n}_T(\omega_0)\sqrt{mn}\bar{\rho}^{(m-1,n-1)}(t) \end{aligned} \tag{1}$$

Here, m, n indicate specific motional elements in $\bar{\rho}$ that represents the entire trapped ion quantum system including spin and motional states. The equation also depends on the system Hamiltonian H'_S which describes the evolution of entire quantum system. Since H'_S depends on the settings of laser, we can set (i.e. conditioning) some parameters on it. We consider 3 kinds of settings, the carrier transition, the blue side band transition and the red side band transition. For each of them, we can get the representation of H'_S.

$$H'_S = -\frac{i}{2}\left[e^{i\eta(c^\dagger e^{i\nu t} + ce^{-i\nu t})}e^{-i\delta t}(e^{i\phi}\Omega)|0\rangle\langle 1| + c.c\right]$$

We've set the phase $\phi = 0$. The lamb-Dicke parameter η is given as some constant which is determined by the experimental setup. The detuning was set $\delta = \nu$ for blue side band transition and $= -\nu$ for red side band transition. The line shifted resonance frequency ν is also set as some constant corresponds to our experimental setup.

Finally, we get the final ordinary differential equation (ODE) (1) which describes the evolution of internal spin states of our quantum system, given the system hamiltonian H'_S and corresponding motional modes m, n. It still looks hard to solve it in closed form, but we can easily solve it numerically. And we can further use such numerical method to infer the important parameters like $\Gamma\bar{n}_T$, which is called as the heating rate, shown in equation (1) by fitting the solution of our ODE solver with those parameters. We've used Euler method to simulate our quantum system with some given initial conditions and parameters. And then for the inferring problem, we've used ODE solver of SciML in Julia using

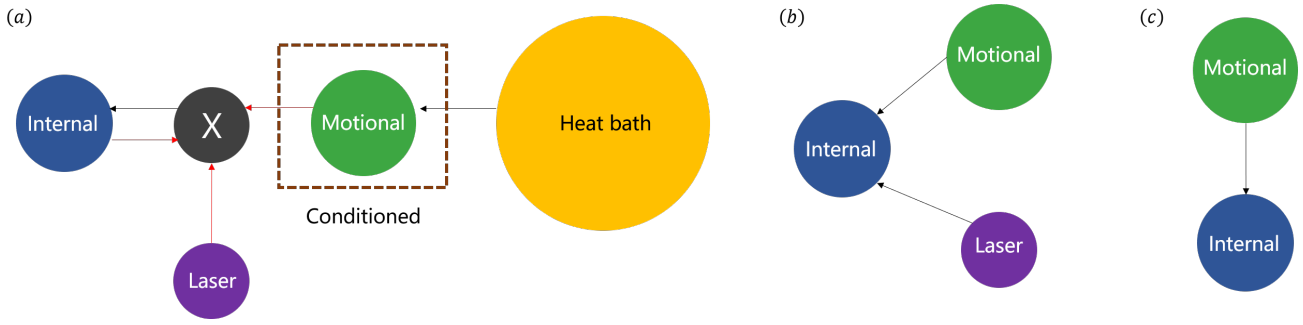

Figure 2. (a) The graphical model conditioned on motional states results in 2 v-structures. The remaining active paths are from Motional state to Internal spin state and from Laser to Internal Spin state (b) The final graph structure derived from figure (a). The node X is marginalized out (c) By enforcing some conditions on the laser setup, the final graphical representation indicates that the evolution of spin states is determined by the corresponding motional states.

AutoTsit5 method to solve our differential equation. We've also used the CurveFit package in Julia to fit the parameters of our equation using the real experimental data.

3. Experiments

3.1. Numerical Simulation of System Dynamics

The numerical simulations results of the carrier, red- and blue-sideband transitions under a heating rate of 2000/s with different initial conditions are presented in Figure 4. The carrier transitions (a) shows the typical decaying behavior. The blue- and red-sidebands (c) and (d) also exhibit expected patterns, the former decaying more quickly and the latter growing larger with increasing initial motional number. In (b) we also plot the population evolution of the individual motional states, which are obtained by marginalization over the internal state degree-of-freedom. Such information is not tractable and usually assumed as a given at a particular instance of time when using the standard methods provided in the Methods section, but can be incorporated into the inference procedure explained in the following section.

3.2. Application to Real Data

Using the numerical simulation, we can calculate the expected internal state for each time step, given a parameter set: Γ, Ω, and $\bar{n}_0$, which is the initial average phonon number of the ion. Therefore, we tried to fit this simulation model to our real experimental data as shown in Figure 5. For more stable fitting, we first fitted the model in Fourier space. Since the output is oscillating over time, it might be unstable to find the optimal parameters with sparse data points, including the oscillation frequency. In Fourier space, a frequency change appears as a peak shift, which will allow more stable fitting. After finding optimal frequency, we then fit the model to the original data, fixing the frequency. We then calculated the heating rate from the fitted parameters, and in Figure 5, it was nearly 300 /s.

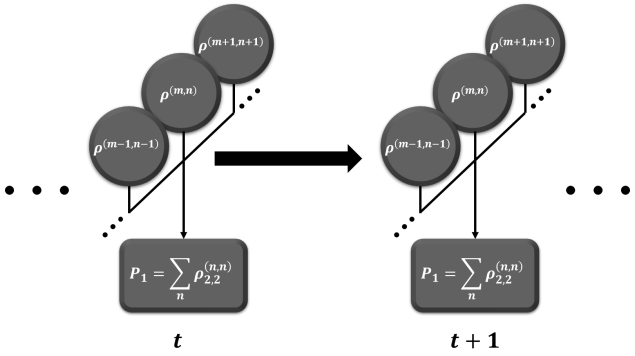

Figure 3. The graphical model that depicts the evolution represented in equation (1). The real data we can observe is the probability that the spin state is 1. The time evolution is determined by some parameters in that equation, so we can fit those parameters with observed data $P_1(t)$ and infer some important statistics of the hidden motional states using them.

4. Conclusion

4.1. Discussion

We have applied a PGM approach to simulate the complicated dynamics of a damped trapped-ion qubit. A directed acyclic graphical model was built to represent the conditional relations among the components that affect the internal state of a trapped ion. The graphical model has shown a very concise and intuitive picture of the system, providing dependency information between the components. Exploiting this information, we were able to establish proper equations step by step in order to reveal the internal state evolution under the motional damping.

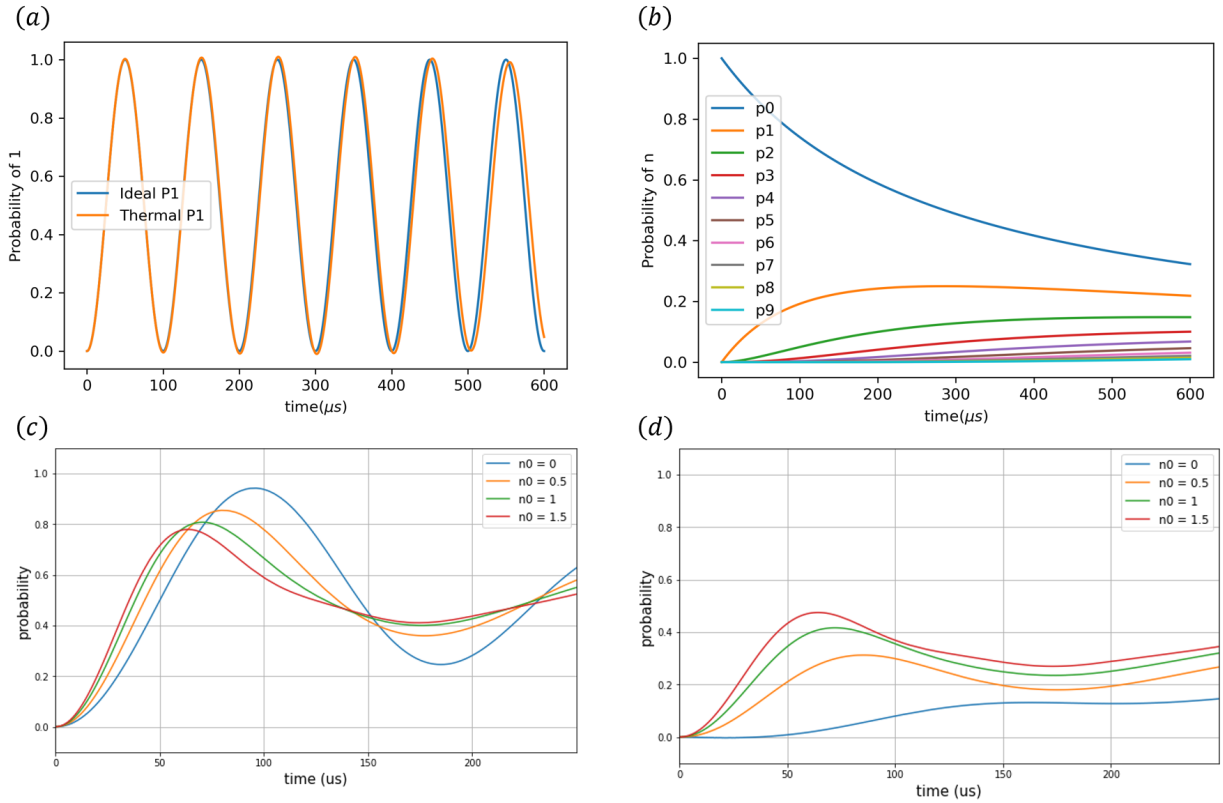

Figure 4. (a) The simulation result of Carrier transition for time evolution of probability that the internal spin states is $|1\rangle$. It is computed by summing up the $(2, 2)$ elements of $\rho^{(n,n)}$ matrices for each time step as $P_1 = \sum_n \rho_{2,2}^{(n,n)}$. As times goes on, the evolution with thermal effect (orange line) starts to oscillate slowly, and the damping of probability can be observed. (b) The time evolution of hidden thermal states $p_n = tr(\rho^{(n,n)})$. It initially have only the zero phonon mode ($p_0(t = 0) = 1$) but it slowly gets higher number of mean phonons due to the thermal effect of Heat bath. (c) The simulation result of Blue side band transition. Corresponds to the theoretical prediction, it oscillates with smaller frequency scaled by the Lamb-Dicke factor ($\eta = 0.1$). Compared to (a), it's frequency scaled about 1/10. (d) The red side band transition. If there's no thermal effect, there should be no oscillation (i.e. transition) at all theoretically. However, due to the effect of Heat bath, the transition starts to occur.

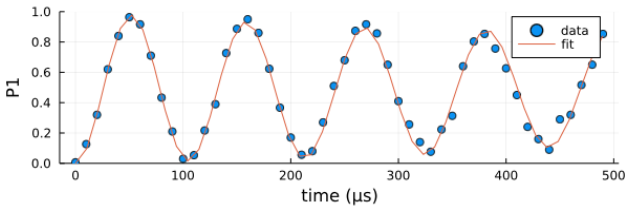

Figure 5. The result of fitting the parameters of our equations to real experimental data. The data is collected by chip-trap based trapped ion quantum system. Blue circles represents the data points and the red line shows the evolution of the probability that spin states is $|1\rangle$. The fitted line is obtained by solving the ODE using obtained parameters. The evolution predicted by our equation fits well on the real data.

4.2. Future work

In this work, the complicated dynamics involving the interactions of the internal and motional degrees-of-freedom coupled to external laser signals and a heat bath has been simplified by a formulation based on the PGM approach. The internal and motional states are propagated through time without loss of information, and then selectively traced out in order to perform marginalization of a variable on demand. The model has been successfully applied to experimental data, extracting the heating rate from the carrier transition only. This is advantageous to standard methods that require both red- and blue-sideband operations and approximate formulas. Our model can also be viewed as a hidden state model, where the motional states are the hidden states and the internal states are the observables, for each time step. The model can be further extended to cover a linear ion

chain, in which multiple ions are trapped along a linear axis. Although the approach developed in our work is not difficult to extend in terms of programming, the computational cost grows rapidly with the number of motional states involved in the simulation. The dimension of the motional and internal states space grows, thus the computational cost for the simulation grows exponentially. It is thus a high priority to find a way to optimize calculations in order to scale up efficiently. One should carefully handle these issues to extend the model to the linear ion chain case.

References

Blatt, R., Ertmer, W., Zoller, P., and Hall, J. L. Atomic-beam cooling: A simulation approach. *Phys. Rev. A*, 34:3022–3033, Oct 1986. doi: 10.1103/PhysRevA.34.3022. URL https://link.aps.org/doi/10.1103/PhysRevA.34.3022.

C. Monroe, D. M. M., King, B. E., Jefferts, S. R., Itano, W. M., Wineland, D. J., and Gould, P. Resolved-sideband raman cooling of a bound atom to the 3d zero-point energy. *Physical Review Letters*, 75(4011), 1995.

Cirac, J. I., Parkins, A. S., and Zoller, P. Quantum collapse and revival in the motion of a single trapped ion. *Physical Review A*, 49(2):1202–1207, 1994.

Dum, R., Zoller, P., and Ritsch, H. Monte carlo simulation of the atomic master equation for spontaneous emission. *Phys. Rev. A*, 45:4879–4887, Apr 1992. doi: 10.1103/PhysRevA.45.4879. URL https://link.aps.org/doi/10.1103/PhysRevA.45.4879.

Gammelmark, S., Mølmer, K., Alt, W., Kampschulte, T., and Meschede, D. Hidden markov model of atomic quantum jump dynamics in an optically probed cavity. *Phys. Rev. A*, 89:043839, Apr 2014. doi: 10.1103/PhysRevA.89.043839. URL https://link.aps.org/doi/10.1103/PhysRevA.89.043839.

Goetsch, P., Graham, R., and Haake, F. Microscopic foundation of a finite-temperature stochastic schrödinger equation. *Quantum and Semiclassical Optics: Journal of the European Optical Society Part B*, 8(1):157–166, feb 1996. doi: 10.1088/1355-5111/8/1/012. URL https://doi.org/10.1088/1355-5111/8/1/012.

Leibfried, D., Meekhof, D. M., King, B. E., Monroe, C., Itano, W. M., and Wineland, D. J. Experimental determination of the motional quantum state of a trapped atom. *Physical Review Letters*, 77(21):4281–4285, 1996.

Mollow, B. R. Pure-state analysis of resonant light scattering: Radiative damping, saturation, and multiphoton effects. *Phys. Rev. A*, 12:1919–1943, Nov 1975. doi: 10.1103/PhysRevA.12.1919. URL https://link.aps.org/doi/10.1103/PhysRevA.12.1919.

P. Zoller, M. M. and Walls, D. F. Quantum jumps in atomic systems. *Physical Review A*, 35(1), 1987.

R. J. Epstein, S. S., Leibfried, D., Wesenberg, J. H., Bollinger, J. J., Amini, J. M., Blakestad, R. B., Britton, J., Home, J. P., Itano, W. M., Jost, J. D., Knill, E., Langer, C., Ozeri, R., Shiga, N., and Wineland, D. J. Simplified motional heating rate measurements of trapped ions. *Physical Review A*, 76(033411), 2007.

Srinivasan, S., Downey, C., and Boots, B. Learning and inference in hilbert space with quantum graphical models. In *Proceedings of the 32nd International Conference on Neural Information Processing Systems*, NIPS'18, pp. 10359–10368, Red Hook, NY, USA, 2018a. Curran Associates Inc.

Srinivasan, S., Gordon, G. J., and Boots, B. Learning hidden quantum markov models. In *AISTATS*, 2018b.

Strunz, W. T. Stochastic path integrals and open quantum systems. *Physical Review A*, 54(4), 1996.

Weiss, T. and Romero-Isart, O. Quantum motional state tomography with nonquadratic potentials and neural networks. *Physical Review Research*, 1.3(033157), 2019.

Zoller, P. and Gardiner, C. W. Quantum noise in quantum optics: the stochastic schrödinger equation, 1997. URL https://arxiv.org/abs/quant-ph/9702030.

Zoller, P., Marte, M., and Walls, D. F. Quantum jumps in atomic systems. *Phys. Rev. A*, 35:198–207, Jan 1987. doi: 10.1103/PhysRevA.35.198. URL https://link.aps.org/doi/10.1103/PhysRevA.35.198.